International Journal of Impact Engineering 99 (2017) 58–68

Contents lists available at ScienceDirect

International Journal of Impact Engineering

journal homepage: www.elsevier.com/locate/ijimpeng

Effect of composite covering on ballistic fracture damage development in ceramic plates

Dennis B. Rahbek[a,*], Jeffrey W. Simons[b], Bernt B. Johnsen[a], Takao Kobayashi[b], Donald A. Shockey[b]

[a] Norwegian Defence Research Establishment (FFI), P.O. Box 25, NO-2027 Kjeller, Norway
[b] Center for Fracture Physics, SRI International, 333 Ravenswood Avenue, Menlo Park, CA 94025, United States

ARTICLE INFO

Article History:
Received 4 May 2016
Revised 15 September 2016
Accepted 18 September 2016
Available online 30 September 2016

Keywords:
Ballistic
Ceramic armor
Cracking
Composite
Modeling

ABSTRACT

This paper describes the damage development in ceramics with and without composite cover during ballistic impact. This is relevant for ceramic inserts in body armor that are often covered with a composite material. To study the effect of the cover on the damage development in the ceramic, projectile impact experiments were performed at sub-muzzle velocities on bare alumina tiles and plates covered with a fiberglass composite. In addition to the experiments, finite element simulations were performed. An atypical formulation was used; Arbitrary Lagrangian–Eulerian (ALE) for the projectile and Lagrangian for the ceramic target. For the ceramic target, an unconventional material model was chosen; the pseudo-geological model 72_R3 in LS-DYNA.

Cracking damage in the recovered plates was characterized in a manner that clearly distinguished between cracking mechanisms and allowed the cracks to be tracked and quantified. In light of the common use of composite cover for ceramics in body armor, an unexpected result was found; that the covered plates showed significantly more damage than the bare plates. The simulations successfully matched details of the cracking patterns and elucidated the damage evolution in the ceramic plates. The simulation results explained the damage observations as the result of restraining effects, i.e. the restraining effect of the composite cover keeps the damaged ceramic in the path of the projectile resulting in increased damage.

1. Introduction and background

Ceramics are attractive tile materials in body armor systems because of their low density and high hardness. The role of the ceramic tile, usually alumina, boron carbide or silicon carbide, is to blunt, shatter, and erode the projectile. The tile is often covered by a composite material, which acts to confine the ceramic fragments and thus improve the multi-hit performance. The ceramic is also often backed with materials capable of absorbing and dispersing kinetic energy. For example, small-arms protective insert (SAPI) plates are often backed with several layers of aramid and/or ultra-high molecular weight polyethylene (UHMWPE) to enhance personal protection.

New designs are continuously sought to improve penetration resistance. Many researchers have performed experiments and developed models in efforts to better understand how ceramic tiles fail, and how failure is affected by a composite cover [1,2,4–16]. The studies do not fully agree on how the performance changes with addition of a composite cover to a ceramic tile. Some studies have shown a positive effect in terms of ballistic performance on an areal density basis of covering ceramic tiles in fiber composites (glass or carbon fibers) or ballistic fibers (aramid or UHMWPE). Sarva et al. studied the ballistic performance of both bare ceramic tiles and tiles with several types of cover material [7]. The study showed significant improvements in ballistic performance and higher projectile erosion (i.e. damage) when adding a front cover and minor additional improvements when also adding a back cover. The increase in performance was attributed to an increased flow of ceramic debris against the projectile due to constraints from the front cover. Contrary to the observations by Sarva et al., Crouch and coworkers [8] have found that adding a composite cover layer to a boron carbide ceramic tile, does not have a significant effect on projectile erosion. This is interesting, since erosion of the projectile is an important mechanism for defeating such threats. In another study, Nunn and coworkers [6] have found a $>40\%$ increase in the ballistic limit, V_{50}, of a boron carbide tile by adding a composite cover that led to an increase in areal density by 9%.

* Corresponding author.
E-mail addresses: dennis-bo.rahbek@ffi.no, dbrahbek@gmail.com (D.B. Rahbek).

http://dx.doi.org/10.1016/j.ijimpeng.2016.09.010

Crouch has shown that the addition of an aramid fiber based cover to a ceramic plate results in a lowering of the back-face deformation upon multi-hit [16]. In the same study, Crouch observed that the addition of the aramid-reinforced composite cover affected the failure mechanisms of the ceramic - an increase in the number of radial cracks in real-sized ceramic SAPI plates from an average 10.8 without cover to 16 was observed when the ceramic was covered. In another study, Reddy et al. [10] found that the size distribution of the ceramic debris created during impact changed toward smaller fragment sizes when a ballistic fiber front cover was added (the ceramic was backed by fiberglass composite).

Most of the above-mentioned impact studies are performed using regular projectiles, including armor piercing (AP) projectiles, or cylinders of similar size as penetrator and impact velocities around muzzle velocity (800–900 m/s) or at even higher velocities. There is, however, also insight to be gained by studying impact at sub-muzzle velocities. For example, Öberg et al. [17] compared the energy absorption of bare and composite backed ceramic tiles using 8 mm diameter steel spheres at 220 m/s. They found that the composite backing increased the energy absorption and that the effect was more pronounced with higher adhesion between ceramic and composite. In another study, Compton and coworkers [3] were able to identify the sequence of failure modes occurring in a ceramic tile by comparing analytical and numerical studies to impact experiments of metal spheres onto confined ceramic tiles in the velocity range of 250–800 m/s.

To better understand test results and to investigate the effects of composite covers on ceramic armor tiles, finite element analyses have been reported in the literature [8,9,11,12,18–24]. In addition to bare and covered ceramic tiles, layered armors, where two or more different materials form a layered structure, and composite armors have been modeled. Many of these analyses were performed with commercial codes using explicit Lagrangian formulations. To lower computational time, symmetry is often exploited in such analyses, sometimes to the extent where 2D simulations are performed to study the impact dynamics [8,20,22,24]. By performing 2D simulations in LS-DYNA, Feli and coworkers [20] found that when a projectile hits a ceramic/composite target, a ceramic cone breaks from the tile and the semi-angle of the conoid formed in the ceramic decreases with increasing impact velocity. The ceramic was modeled using the Johnson-Holmquist 2 (JH2) material model [23]; one of the most commonly used material models for ceramics.

Due to the non-symmetric nature of damage (cracking patterns) observed in ceramics, a full 3D approach (or applying half/quarter symmetry) is often required to describe the dynamics of the problem. A full 3D geometry was used by Grujicic et al. [21] to study the role of the adhesive interlayer between a ceramic tile and a composite back layer, using the JH2 model for the ceramic. The results showed that by adjusting the material properties of the adhesive, the performance of the hybrid armor can be improved. However, the study also showed that material properties that result in the best single-hit performance not necessarily optimize multi-hit performance. This is in line with results from other studies, showing that optimum thickness of the interlayer is a compromise between lowering either ceramic damage or back plate deformation [12] and that the damage accumulation of the ceramic is affected by the choice of interlayer material [11]. Bürger et al. [18] have also modeled projectile impact on a ceramic/composite target using the JH2 material model for the ceramic. The simulations were able to reproduce ballistic limits, V_{50}, found experimentally. However, the JH2 ceramic model was not able to reproduce the failure mechanics. The simulations showed less damage to the ceramic than what was observed experimentally.

The analyses mentioned above used Lagrangian continuum codes in which material damage was typically modeled by eroding (i.e. removing from the model) elements that have reached full damage. For ceramic armor, eroding elements can have significant effects on the ballistic response of the ceramic because the strength of the ceramic depends on the level of confinement; more confinement gives higher strength. By eroding elements, confinement is reduced and the adjacent elements in the ceramic lose strength and modify the stress field. As a result, fracture patterns observed experimentally are often not accurately reproduced. Alternative formulations have therefore been developed to better capture the response of fractured elements and to capture fracture patterns. Riedel et al. [25] combined commercial and in-house developed codes and material models, including a smoothed particle hydrodynamics (SPH) approach, to analyze fracture patterns and post-fracture loading for different loading histories, as well as failure conditions for edge-on impact experiments in ceramics. Eghtesad et al. [26] developed a corrective smoothed particle method (CSPM) modification of the traditional SPH method to predict fracture and fragmentation in ceramics under hypervelocity impact conditions. Espinosa et al. [27,28] developed an approach using a material model for cracking based on a multiplane plasticity approach that tracks crack initiation and growth in an element combined with a brittle fracture model to form discrete fragments that can interact.

In the present paper, ballistic experiments on bare and covered alumina tiles are described. A fiberglass composite is used for covering the tiles. These materials were chosen as they are commonly

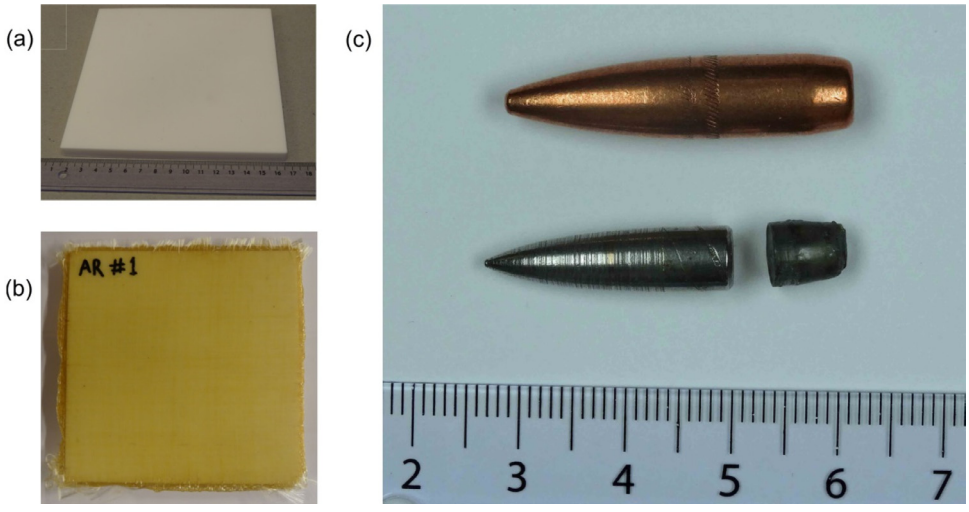

Fig. 1. (a) Bare ceramic tile, (b) ceramic tile covered with fiberglass, and (c) the M61 7.62 mm AP projectile with the steel core and lead filler shown individually.

used for ballistic protection and commercially available. The scope of this work is not to study the effect a composite cover has on the ballistic performance of a ceramic tile, but to study how the addition of a composite cover affects the damage mechanisms in the ceramic tile. To allow for post damage analysis, without having to add additional ballistic fiber backing materials to support the ceramic, the impact velocities were restricted to sub-muzzle levels. Depending on the impact velocity, differences in fracture damage are observed and described. The experimental results are compared to finite element modeling results that were performed in LS-DYNA using a combination of Lagrangian and Arbitrary Lagrangian–Eulerian (ALE) formulations. An unconventional material model for ceramic, employing non-eroding elements, is used to provide additional information about the fracture damage and the effect of the composite cover.

2. Materials and experimental methods

Bare alumina tiles and tiles covered with a fiberglass composite were impacted with M61 7.62 mm AP projectiles at sub-muzzle velocities. Fig. 1 shows images of the targets and the projectile. The M61 7.62 mm AP projectiles consist of a 3.7 g hardened steel core, a 1.8 g lead filler behind the steel core, and a 4.3 g copper jacket for a total mass of 9.8 g. The Alotec 98 SB alumina tiles, obtained from CeramTec (Plochingen, Germany)[1], were 151 mm on two sides and 10 mm thick, and have material properties as listed in Table 1.

Six tiles were covered with a woven, balanced twill (2/2), fiberglass/low-melting temperature polyethylene terephthalate (LPET) fabric, WG1-LPET-750, provided by Comfil (Gjern, Denmark). Two layers were added to both the front and the back of the ceramic tile without any surface treatment, resulting in an increase in the areal density by 7.7% from 39.1 to 42.1 kg/m^2. The covered tiles were then heated in vacuum at 210 °C for 90 min, during which the polymer melted, infiltrated the glass fibers, and formed a consolidated matrix when cooled. The density of the consolidated composite was 1.87 g/cm^3. In previous studies [29,35], this production method was found to result in good adhesion between the LPET matrix and the alumina ceramic with an estimated interfacial fracture energy of 2810 J/m^2. The six unwrapped tiles were covered with either a 1 mm thick polyurethane sheet or with four layers of regular packaging tape to maintain their integrity after impact. Because of their low strength, these covers were not expected to influence the damage produced by the impacting projectile.

Ballistic tests were performed at both SRI International and at the Norwegian Defence Research Establishment (FFI). For the tests performed at SRI International, the projectile was accelerated with a gas gun. Reproducible velocities and minimal yaw were achieved by fitting the projectile with a 0.5 g vinyl sabot. The projectile velocities were recorded with high-speed video using a Phantom 7 camera. A mirror inclined at 45° to the camera viewing direction provided perpendicular views of the projectile in flight, so that projectile yaw and pitch could be observed, as shown in Fig. 2. For the tests performed at FFI, a powder gun was used to accelerate the projectile and a laser velocity gauge was employed to measure the velocity. Apart from this, there were no differences in the two test set-ups. In all experiments, the targets were backed by ballistic clay and no yaw or pitch was detected. Six experiments were performed on bare tiles, and six experiments were performed on composite-covered tiles at velocities ranging from 176 to 351 m/s. In this velocity range, the impact event resulted in substantial cracking damage to the ceramic, however, not to such a degree that the damage was unquantifiable.

[1] According to the manufacturer, the density was 3.80 g/cm^3. However, we measured 3.91 g/cm^3.

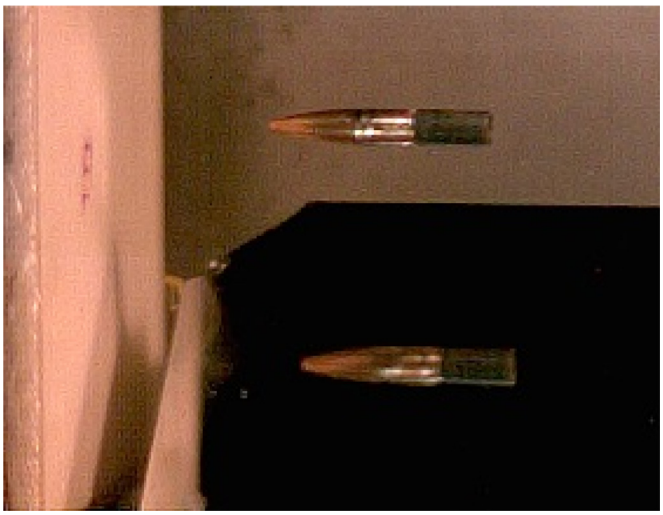

Fig. 2. An M61 7.62 mm AP projectile in flight prior to impacting the target on the left. The two images taken at 90° to each other via a mirror show no yaw or pitch of the projectile.

Table 1
Properties of Alotec 98 SB alumina (as provided by the manufacturer).

Property		Unit	Value
Density	ρ	g/cm^3	3.80
Residual porosity	p	%	<2
Median grain size	D	μm	6
Vickers hardness	HV (5)	GPa	13.5
Young's modulus	E	GPa	335
Bending strength	σ_b	MPa	260
Fracture toughness	K_{Ic}	MPam$^{1/2}$	3.5
Sound velocity	V_L	km/s	10.2

After ballistic testing, a red dye penetrant (Bycotest RP20) was applied to the impacted surface of the targets. The penetrant infiltrated the cracks and made them more visible. The cracked tiles were then stabilized by soaking them in a low-viscosity epoxy (Buehler EpoThin) and allowing the epoxy to cure overnight at room temperature. After curing, the fiberglass was removed from the covered targets and the cracking patterns on the front and back sides were examined. The targets were then sectioned through the shot line using a circular water-cooled diamond blade saw, and the cross-sections were examined visually and with optical microscopy.

3. Ballistic test results

The results of two bare (B176 and B299) and two covered (C188 and C317) targets are discussed in detail here. (The letter “B” or “C” in the target identification indicate bare or covered target, respectively, while the number indicates the measured impact velocity.) These four experiments, specified in Table 2, are representative of the other eight experiments as the damage in the targets all showed the same trends in damage with velocity and with covering.

Two main damage mechanisms were observed in the tests: 1) radial cracks and 2) cone cracks. Fig. 3 shows three views of target B299. The images are combined near the center of the sectioned target, so that the damage on the front side, the cross-section, and the back side are aligned. The radial cracks are observed to extend from underneath the impact point on the front and back sides and outward in a radial direction. The cone cracks are best seen in the cross-sectional view, where they are observed to form a cone extending from the impact point on the front side and spread to the back

Table 2
Details of the four representative impact experiments that were selected for presentation.

Target	Type	Areal density (kg/m^2)	Velocity (m/s)	Number of radial cracks	Cone cracks
B176	Bare	39.1	176	6	Some
B299	Bare	39.1	299	9	Yes
C188	Covered	42.1	188	10	No
C317	Covered	42.1	317	14	Yes

surface. The extents of these two failure modes are quantified and summarized in Table 2.

The extent of damage on the back side of the four ceramic targets, as shown in Fig. 4, increased with increasing velocity for both bare and covered targets. At lower velocities, the damage was primarily radial cracks for both the bare (Fig. 4a) and covered (Fig. 4c) targets. At higher velocities (Figs. 4b and 4d), cone cracks intersected a higher number of radial cracks. Radial cracks were also visible on the front side of all the targets, as shown in Fig. 5, indicating that most of the radial cracks extended through the entire thickness of the ceramic.

Increasing the impact velocity for the bare targets from 176 m/s (B176) to 299 m/s (B299) increased the number of radial cracks from 6 to 9. Only a slight indication of cone cracking was observed at the lower velocity. However, cone cracking was extensive at the higher velocity. The diameter of the cone-cracked area at the back of the tile was on average 69 mm in the bare targets.

A similar increase in the extent of damage with impact velocity was observed in the covered tiles. The number of radial cracks increased from 10 to 14, and while no cone cracking was observed at the lower velocity (C188), extensive cone cracking occurred at the higher velocity (C317). There was no significant difference in the size of the cone-cracked region between the bare and the covered ceramic.

For both the bare and the covered ceramic, the radial cracks in the cone region are connected by transverse cracks. However, the degree of fracture damage inside the cone region is different for bare and covered ceramic. The covered ceramic exhibit additional radial cracks in the cone region as well as a network of cracks between the radial cracks. The density of cracks in the cone region is therefore much higher in the covered tile and, hence, a much higher number of incipient fragments are formed in the covered targets. Thus, at the higher velocity where the cone region was formed, the ceramic tiles that were covered with fiberglass sustained more back-face damage than the bare tiles.

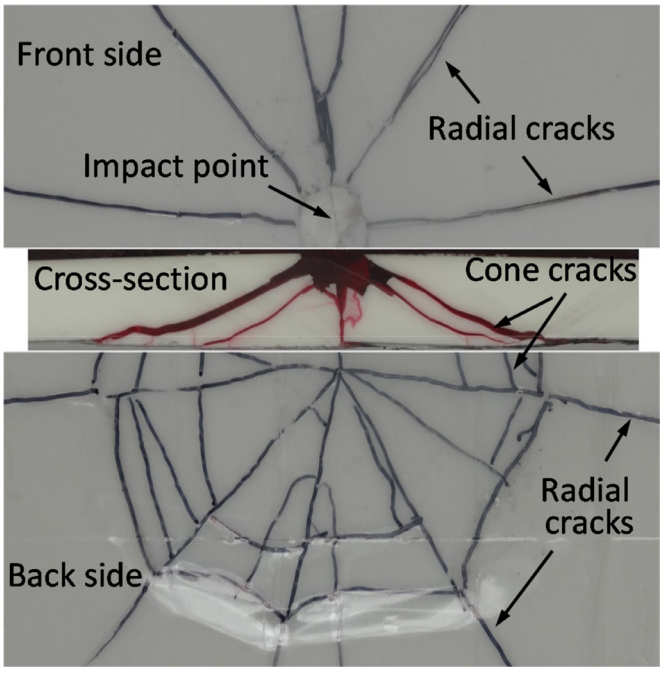

Fig. 3. Types of ceramic damage observed in the targets.

The same trend is seen on the front side and on cross-sections taken through the shot line, as seen in Fig. 5. The dense cracking that was observed on the back side of the covered ceramic is also visible on the cross-section of the tile. For example, a significant number of fine cracks extend up from the back side of the ceramic, some of which are arrested inside the ceramic, while others extend all the way to the cone cracks. These cracks are in many cases bifurcated, a behavior not observed for bare tiles. Thus, the front side, cross-section, and back side images clearly differentiate the type and extent of damage in bare and covered ceramic tiles.

Another observation is that, for the bare ceramic, the cracking pattern on the cross-sections shows substantial gaps, which are 2–3 mm in width, between the displaced cone and the remaining material. In addition, the radial cracks on the tile surface appear as vertical cracks beneath the impact region. For the covered ceramic, the separation between the cone region and the remaining material is much smaller. In both cases, however, there seems to be a tendency for the formation of two or more cone cracks, extending at slightly different angles, from the point of impact toward the back side of the tile.

The projectiles were severely damaged during the tests. In most of the tests, the tip of the hardened steel core shattered into small pieces and the copper jacket was plastically deformed, see Fig. 6. The damage to the steel core (erosion of the front of the core) was observed to increase with increasing impact velocity. However, no significant difference in core damage was observed between impact against bare and covered tiles. In the region around the impact zone, some delamination between the two fiberglass layers was observed. Except for this delamination at the impact region, the fiberglass cover did not appear to be damaged in any of the covered targets.

4. Modeling

3D finite element simulations were performed using the commercial software LS-DYNA [32]. Two bare targets and two covered targets were simulated at velocities of 200 and 300 m/s to enable direct comparisons between bare and covered targets in the model and to the experimental findings in Fig. 4. Because the cracking pattern in the targets was not symmetric, no planes of symmetry were assumed in the model, and the target and projectile were modeled as shown in Fig. 7a, with a quarter cross-sectional close-up view of the projectile model shown in Fig. 7b.

A finite element formulation was used compared to the formulations described above. A Lagrangian element formulation was used for the target, clay and aluminum box, however, without removing failed elements. Because of the large deformations experienced during the impact, the projectile was modeled using an ALE formulation that included the copper jacket, hard steel core, and lead backing as well as a surrounding air volume to accommodate the ALE formulation. The two formulations were coupled with a constraint condition. Representative mesh resolution is shown in Fig. 8 for the area

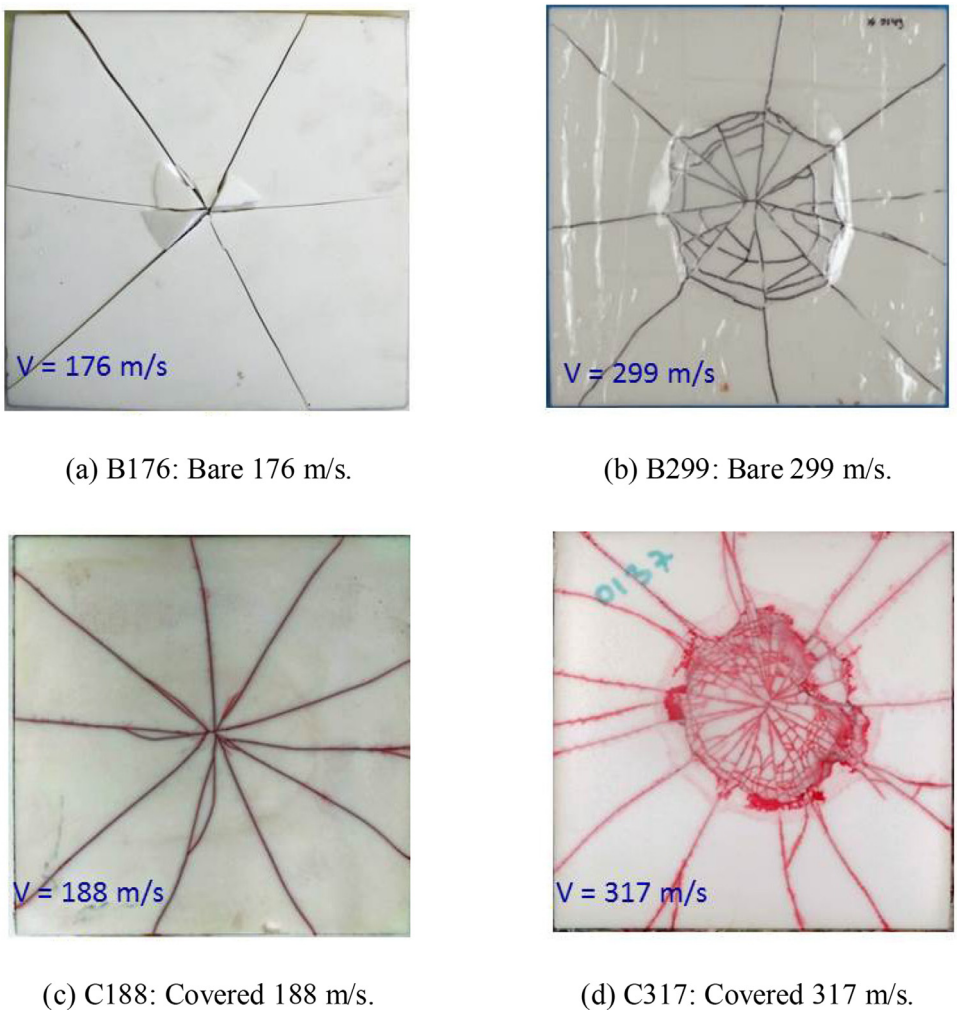

(a) B176: Bare 176 m/s. (b) B299: Bare 299 m/s.

(c) C188: Covered 188 m/s. (d) C317: Covered 317 m/s.

Fig. 4. The back sides of the ceramic targets showing the extent of damage after projectile impact: (a) B176, (b) B299, (c) C188, and (d) C317.

around the projectile impact. Typical mesh dimensions were about 250 μm. The full model contained a total of about 1000,000 elements.

The copper jacket, hardened steel core and lead filler of the projectile were modeled using the Johnson–Cook material model [30,31] with material and failure constants as listed in Table 3. The clay was modeled as an elastic-plastic kinematic material with constants, shown in Table 4, which produced permanent deformations approximately equal to those measured in the experiments (2–4 mm).

The fiberglass on each side was modeled using a 2-element thick layer of elastic elements with density (1.87 g/cm^3) and overall thickness (0.8 mm) consistent with measurements described above, and stiffness and strength properties shown in Table 5 as estimated from test data described in [29]. The fiberglass was connected by a tied interface to the ceramic.

A pseudo-tensor geological model (model 72_R3 in LS-DYNA [32]) was used for the ceramic. This unconventional model was chosen, after trying several others, including the Johnson-Holmquist 2 (JH-2), because of its capability to simulate the damage response mechanisms that were observed in the sub-muzzle velocity tests, including tensile cracking and shear cracking under low confinement stresses, and its capability to accurately model the observed cracking patterns.

Based on specified values for unconfined compressive, f_c, and tensile strength, f_t, shown in Table 6, the pseudo-tensor model determines parameters for the initial strength and failure surfaces as functions of confining pressure, P, of the form

$$S = A_0 + \frac{P}{A_1 + A_2 P} \tag{1}$$

where S is strength and constants A_0, A_1 and A_2 are generated by input quantities f_t and f_c listed in Table 6.

Fig. 9 compares the initial shear strength surface for alumina for the current model based on values of 2.0 GPa for compressive strength and 180 MPa for tensile strength with the JH-2 model for 99.5% alumina. The parameters for the JH-2 model are taken from Cronin et al. [33], with reported values of 2.0 GPa for compressive strength and 200 MPa for tensile strength. Note that because the specified tensile strength is a limit of maximum principal stress it does not show explicitly on this graph. For comparison, the reported bending strength of the alumina of 260 MPa (see Table 3) is greater than the 180 MPa tensile strength specified in the model, which is consistently the case for brittle materials.

Damage in the model is based on λ, the modified effective plastic strain, which is calculated as a function of effective plastic strain, $\bar{\varepsilon}^p$, a strain rate enhancement factor, r_f, and pressure, p, as follows:

$$\lambda = 0 \begin{cases} \int_0^{\bar{\varepsilon}^p} \dfrac{d\bar{\varepsilon}^p}{r_f\left(1 + p/r_f f_t\right)^{b_1}} & \text{for } p \geq 0 \\ \int_0^{\bar{\varepsilon}^p} \dfrac{d\bar{\varepsilon}^p}{r_f\left(1 + p/r_f f_t\right)^{b_2}} & \text{for } p < 0 \end{cases} \tag{2}$$

where b_1 and b_2 are constants.

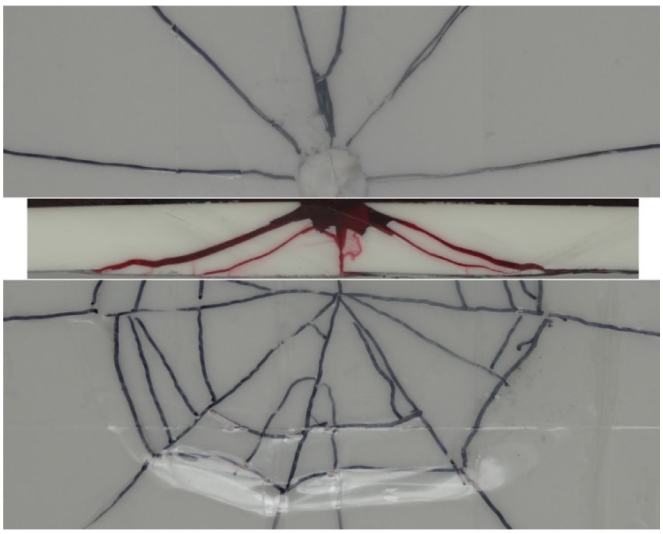

(a) B299: Bare 299 m/s.

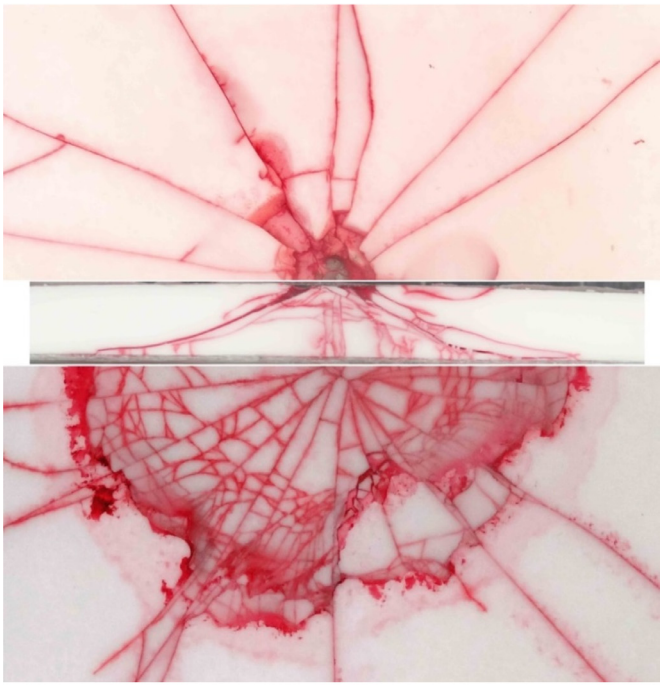

(b) C317: Covered 317 m/s.

Fig. 5. The front side (top), cross-section (middle), and back side (bottom) of (a) a bare tile (B299), and (b) a covered tile (C317).

This formulation allows for brittle damage under low confinement and more ductile damage under high confinement. The damage value, η, calculated by the model as a tabular function of λ as shown in Fig. 10, is used to scale the strength between the initial yield surface (η equals 1) and the failure surface (η equals 0), as shown in Fig. 9. Note that even material that has completely failed can have considerable strength when confined. Details of the model are given in Malvar et al. [34].

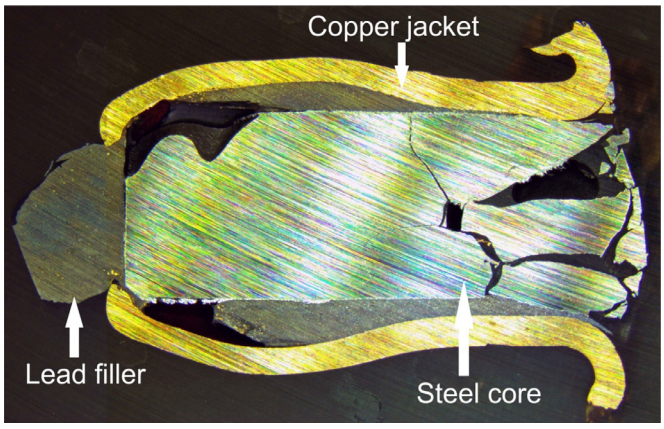

Fig. 6. (a) Projectile after impact at 299 m/s. The projectile has been embedded in epoxy and sectioned.

The volumetric response (i.e., the EOS) is a multilinear function of pressure as a function of volume strain that depends on the compressive strength of the material. The volumetric response for the input constants chosen is shown in Fig. 11.

So although a concrete model may be thought of as having too much porosity to model ceramic, this model is also used to model very high-strength concrete, which typically has very low porosity. For this choice of constants, the pore compaction at 500 MPa is only about 1%, and pressure that high is only reached in elements just under the projectile, i.e., in material that has already fractured in shear and tension.

4.1. Modeling results

Results from the simulations showing cracking patterns in the ceramic are displayed in Fig. 12. The damage, with a scale as described above, 100 μs after impact is shown for the two bare and the two covered ceramics with simulated impacts at 200 and 300 m/s. For both bare and covered ceramics, the number of radial cracks increases with increasing impact velocity, and increasing velocity enhances cone cracking for the bare ceramic, while it "initiates" cone cracking in the covered ceramic. These modeling results are directly comparable to the experimental results shown in Fig. 4. Hence, the same crack patterns as those observed experimentally are also seen in the simulations; through-section radial cracks extending to the edge of the ceramics, cone cracks, and cracks that are connecting the radial cracks inside the cone region. The same trend of an increased number of radial cracks and increasing extent of cone cracking with increased velocity is also seen.

Fig. 13 shows modeling results for damage development on the back side of a bare ceramic tile at an impact velocity of 300 m/s. The modeling shows that the radial cracks are the first to appear on the back side. These are initiated at the center of the target, beneath the

Table 3
Johnson–Cook constants for projectile core, filler and jacket.

	ρ	A	B	n	c	m	$D1$	$D2$	$D3$	$D4$	$D5$
	(g/cm^3)	(MPa)	(MPa)								
Jacket (OHFC copper)	8.96	90	292	0.31	0.025	1.09	0.54	4.98	-3.03	0.014	0.0
Core (4340 steel)	7.80	792	510	0.26	0.014	1.03	0.05	3.44	-2.12	0.002	0.61
Filler (Lead)	11.34	10.4	41.3	0.21	0.0033	1.03	0.25	0.0	0.0	0.0	0.0

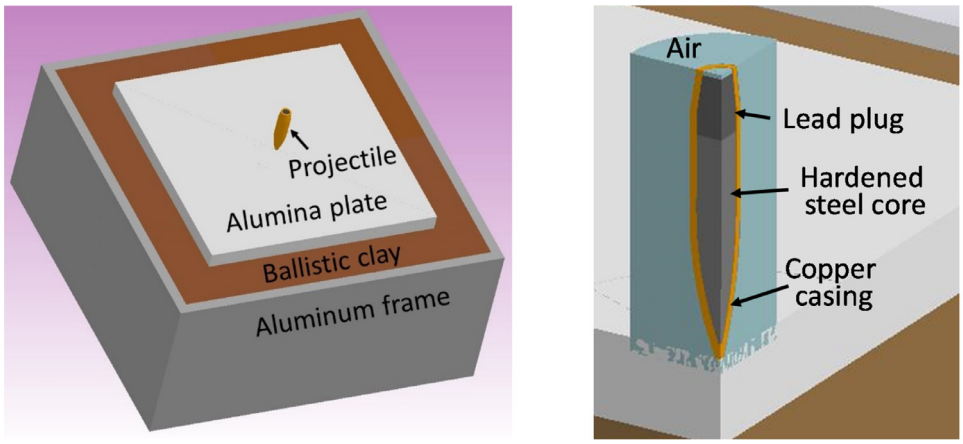

Fig. 7. Model configuration for impact analysis.

Table 4
Elastic–plastic kinematic constants for clay.

	ρ	E	ν	σ_y	E_{tan}	β
	(g/cm^3)	(MPa)		(kPa)	(kPa)	
Ballistic clay	1.57	1.0	0.49	90	90	0.0

Table 5
Elastic constants for fiberglass composite.

	E	ν	ε_{fail}
	(GPa)		(%)
Fiberglass composite	20	0.25	2.5

Table 6
Model 72_R3 constants for alumina.

	ρ	ν	f_t	f_c	A_0	A_1	A_2
	(g/cm^3)		(MPa)	(GPa)	(GPa)		(1/GPa)
Alumina	3.69	0.15	180	2.0	0.621	0.446	0.0385

impact zone, and expand radially outward (Figs. 13a and b). At the time the cone cracks reach the back side of the ceramic tile (Fig. 13c), several of the radial cracks have reached the edge of the target, while other radial cracks have stopped before reaching the edge of the plate. The cone cracks continue to grow, connecting the radial cracks (Fig. 13d). The same process – first radial cracks, then cone cracks – can be deduced from the experimental results in Fig. 4 because the full radial cracks are all continuous across the cone crack boundary, whereas the cone cracks are partly discontinuous across the radial cracks.

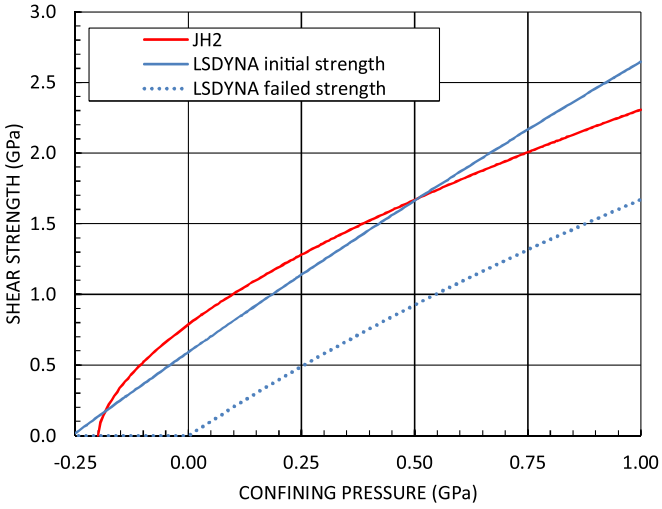

Fig. 9. Model strength surface of alumina under confinement.

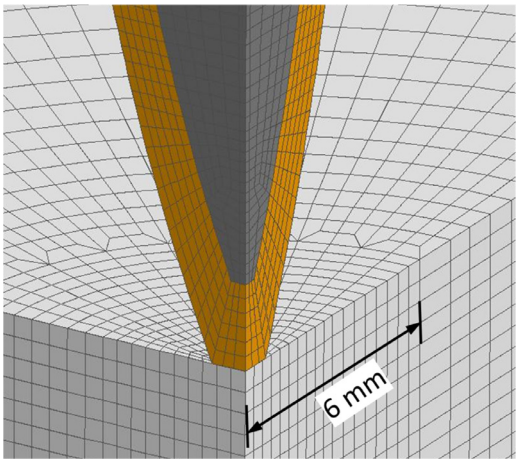

Fig. 8. Representative mesh resolution around the point of impact.

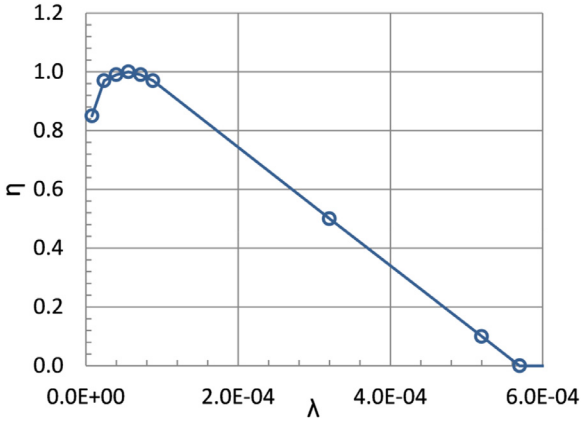

Fig. 10. Damage as a function of modified effective plastic strain λ.

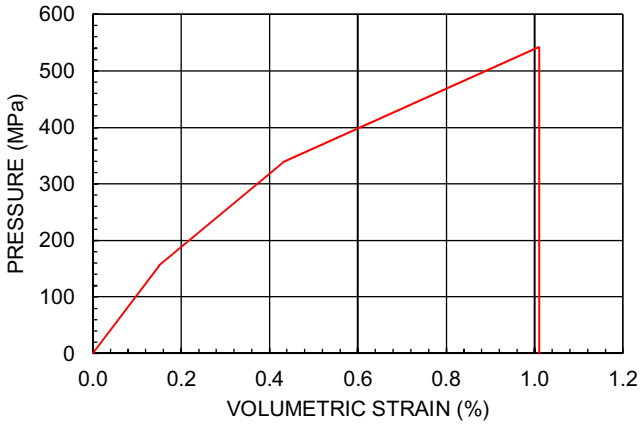

Fig. 11. Volumetric response model.

The damage to the front of the projectile core, i.e. erosion of the core tip, found from the experiments and the model is shown in Fig. 14. Damage to the front of the projectile core for bare and covered targets. Error bars in the experimental results indicate multiple measurements on single projectiles or multiple tests at the same velocity. In either case, there is significant scatter in the measurements. However, the experiment and model show similar trends: 1) projectile core damage increases with increasing velocity, and 2) there is no significant difference in projectile core damage between bare and covered targets.

Fig. 15 shows the calculated rigid body velocity of the projectile, i.e., the velocity of the center of mass, during impact for both bare and covered targets at 200 and 300 m/s. The two projectile velocity curves (bare and covered) at each impact velocity are almost identical from impact at 0 μs to the end of the simulations at 200 μs. Although the covered velocities are slightly lower than the bare velocities at times above 65 μs, the model suggests that the covering has almost no effect on stopping the projectile at these sub-muzzle velocities.

As a whole, the results show that the pseudo-tensor geological model (model 72_R3 in LS-DYNA) successfully captures the ceramic damage mechanisms observed in the experiments. The model correctly reproduces the observed crack types: the radial cracks, the cone cracks, and the connecting cracks between the radial cracks. Moreover, the model predicts an increase in the number of radial cracks with increasing velocity as observed experimentally – both for bare and fiberglass-confined tiles. The increase in damage in the ceramic when covered with the fiberglass composite is also predicted. In addition, the Johnson-Cook model describes the response of the projectile core, which physically erodes as it interacts with the target and, as in the experiment, shows greater erosion at higher velocities and no significant difference in the extent of projectile damage for the bare and covered targets.

5. Discussion

The results presented above show that the damage produced in an alumina tile by an AP projectile for a moderate velocity impact increases when confined by a fiberglass composite. The increase in

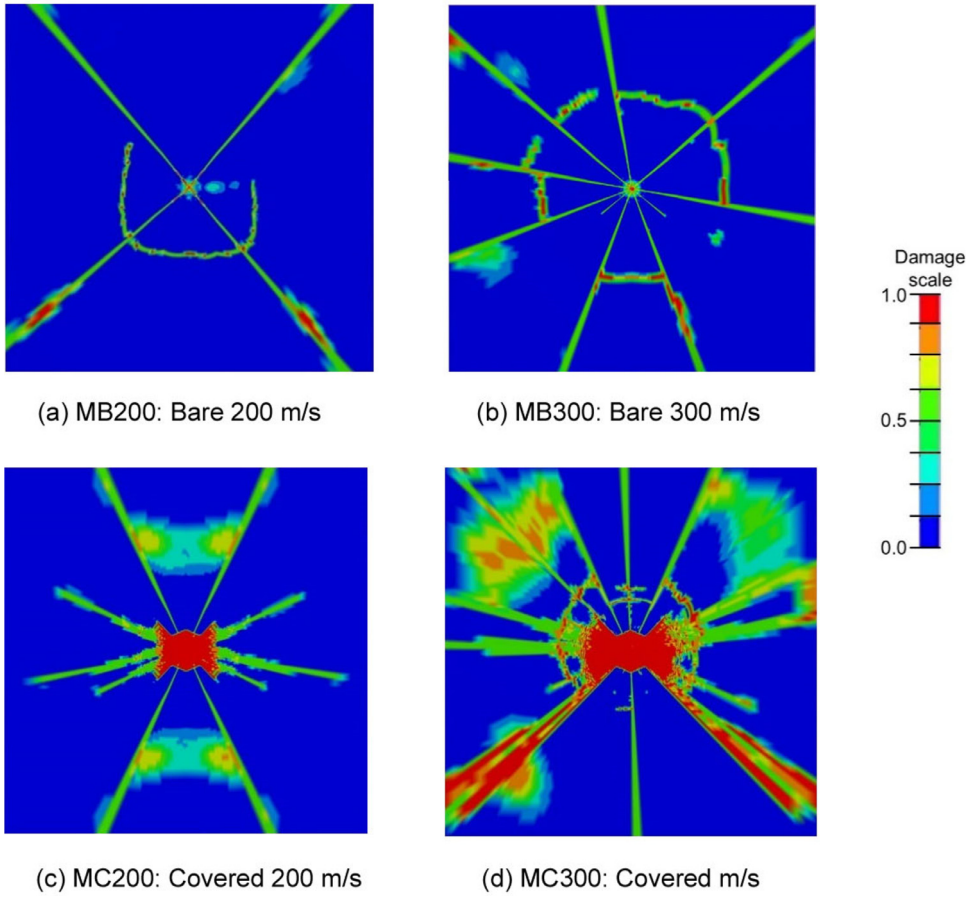

Fig. 12. Model results showing the extent of "damage" on the back side of the ceramic targets 100 μs after projectile impact. (The letter "M" in the target identification indicate "model".).

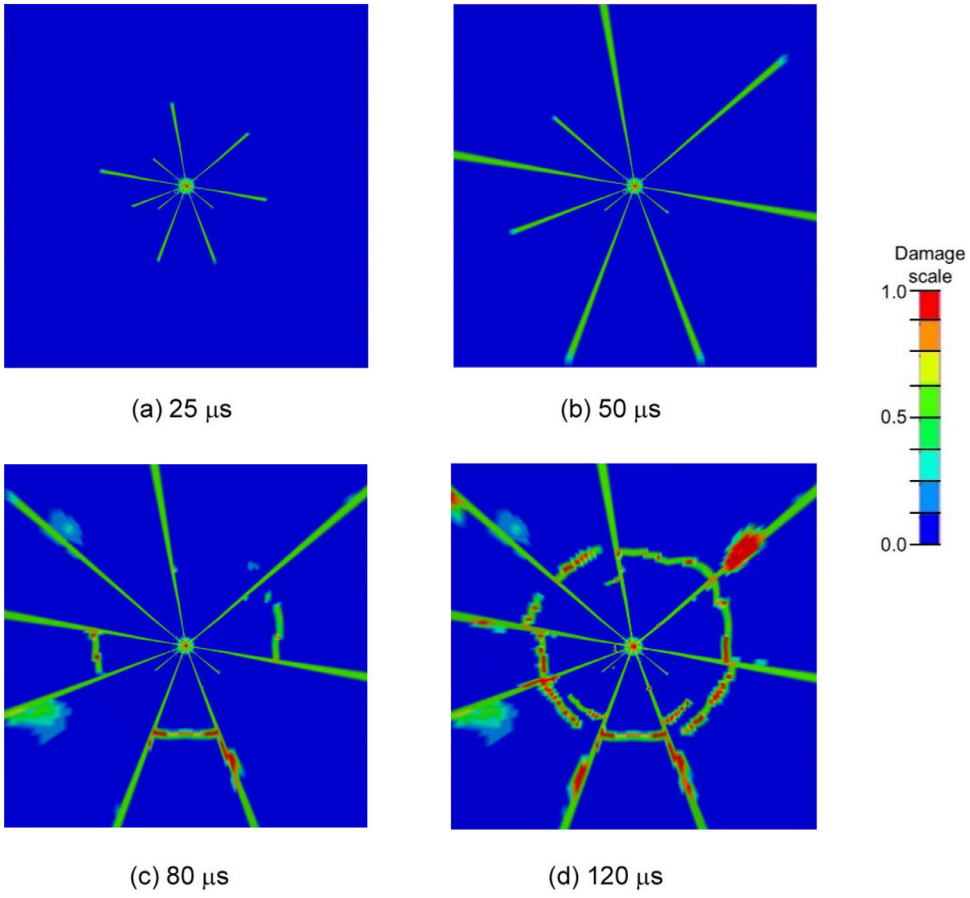

Fig. 13. Damage development on the back side of a bare ceramic tile at an impact velocity of 300 m/s (MB300).

damage is observed as a larger number of radial cracks, but also as a substantial increase in cracking inside the cone region. We note that Crouch [16] also found an increase in the number of radial cracks in ceramic tiles during impact when the ceramic was covered by a fibrous material. In the same work, it was also found that the opening of the radial cracks is smaller for the covered tiles due to the confining effect of the cover material. This is in line with the present work, where the opening of the radial cracks in covered tiles was also observed to be smaller than in bare tiles. An example of this is seen in Fig. 5a, where the vertical crack in the cross-section view (i.e. a radial crack in side view) of an uncovered, bare tile is substantially larger than the corresponding radial crack(s) for a covered tile, seen in Fig. 5b. The confining effect of the cover material at the later stages of the impact process is also observed in the displacement of the cone region, which was roughly 2 mm larger for the bare ceramic than for the covered at an impact velocity around 310 m/s. The simulation successfully reproduced the same response; a significantly larger maximum displacement for a bare tile (3.45 mm at 300 m/s), than for a covered tile (2.81 mm at 300 m/s) due to the restraining effect of the cover material.

From the discussion above, it follows that the main effect of the cover is to keep the cracked ceramic material in the cone region in the path of the incoming projectile, thereby forcing the cracked fragments to continue to interact with the projectile. This, in turn, increases the fragmentation of the ceramic, as can be seen by

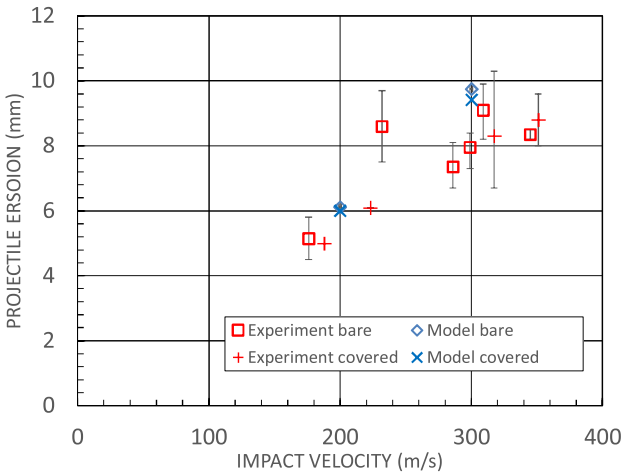

Fig. 14. Damage to the front of the projectile core for bare and covered targets.

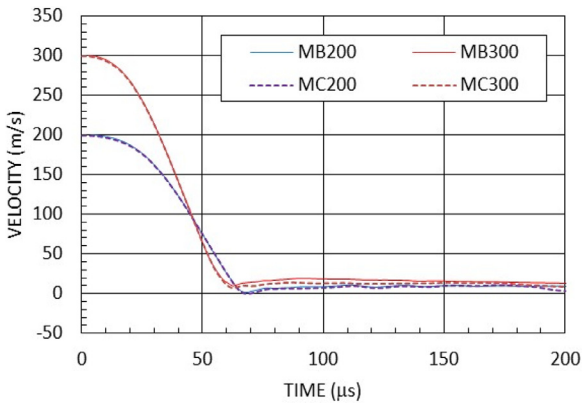

Fig. 15. Calculated projectile velocity for bare and covered target at 200 and 300 m/s.

comparing the cracking between a bare and a covered target, see Figs. 5a and b. This effect of increased damage in the cone region with cover restraint is also successfully reproduced in the modeling results, as seen in Fig. 12.

In support of the work presented here, Reddy et al. [10] also found that adding a cover results in smaller ceramic fragments, while Sarva et al. [7] showed that the plume of ceramic debris that is forced outward against the penetrator during impact is directed more narrowly toward the penetrator when a front cover is added. For this reason, it was suggested that the improved performance of the covered ceramic was due to an increase in ceramic/penetrator interaction. This increase in interaction can also be achieved without a cover, as shown by Sherman and Ben-Shushan [4], by instead adding a lateral confinement (without pre-stress). In any case, it seems clear that some form of restraint imposed on the ceramic will have an effect on both the damage mechanisms and the ceramic/penetrator interaction. It is interesting, however, that no changes in physical erosion of the projectile core were observed in this work when a cover was added to the ceramic. This observation stands in contrast to the results of Sarva and coworkers [7], but fully in line with the findings of Crouch et al. [8], where the addition of a composite cover to a boron carbide tile did not result in additional penetrator erosion. Whether this difference is due to the materials in the penetrator or perhaps the shape of the penetrator tip is unclear, and should be subject to further investigation.

In this study, the impact velocity (176–351 m/s) is much lower than muzzle velocity and, unlike impacts at muzzle velocity on bare and covered tiles [7,10], no penetration of the ceramic by the projectile was observed. Nevertheless, even with no penetration of the projectile into the target, and hence minimal ceramic/projectile interaction, the covered ceramic was much more heavily damaged than the bare ceramic. However, together with the modeling results, these observations suggest that the performance increase observed in some of the studies in the literature [6,7,10,17], is not due to an increase in the performance of the ceramic as such (in terms of improved material properties, or greater resistance to fracture), but instead simply due to the ceramic being forced to remain in the path of the penetrator.

6. Summary and conclusions

Ballistic impact experiments were performed on bare and covered alumina ceramic targets. These tests allowed identification and characterization of the damage mechanisms in the ceramic armor at sub-muzzle velocity. The observed damage mechanisms included radial and cone cracks in the ceramic, as well as fragmentation and erosion of the projectile steel core. These damage mechanisms were also observed in modeling.

As observed in the sub-muzzle velocity experiments and the modeling, the role of a composite cover on resisting projectile penetration is to restrain cracked and fragmented ceramic material from moving away from the region in advance of and around the projectile, which results in more damage to the covered tiles than the bare tiles. At these velocities, which are below those necessary for the projectile to penetrate the targets, more damage to the covered targets is the only significant effect seen. No significant difference is seen in the amount of damage (i.e. erosion) sustained by the projectile between the bare and covered targets, so any measure of armor "performance" at these velocities would be the same for bare and covered tiles. However, the restraining effect of the covering on the ceramic, which results in more damage to the covered ceramic, will also give higher resistance against a penetrating projectile. This complements and broadens the observations by Sarva et al. [7], who suggested that the effect of a covering layer in improving ballistic performance is increased interaction between the projectile and the target.

A finite element modeling approach was developed using an unconventional model choice for the ceramic, the psuedo-tensor material model 72_R3 in LS-DYNA. The ceramic and the rest of the target configuration were modeled with a Lagrangian formulation for the target without eroding failed elements, while the AP projectile was modeled using an ALE formulation using the Johnson-Cook material model.

This combination of formulation and material models was able to capture and provide insight into many of the cracking patterns and responses observed in the experimental tests including: 1) a moderate number (4–12) of radial cracks emanating at seemingly random orientations from the point of impact toward the edges of the target, followed by cone cracks that connect the radial cracks; 2) increasing number of radial cracks with increased velocity; 3) significantly more damage to covered targets than bare targets; and 4) increasing erosion of the projectile with increasing velocity, with no influence by the covering. These responses were not easily or accurately captured by other modeling approaches surveyed.

7. Future work

The major findings in this investigation are that: 1) the main effect of covering in composite ceramic armor is to keep fractured ceramic in front of the penetrator resulting in increased cracking to covered tiles, and 2) an advanced finite element model was developed that accurately reproduced the extent and patterns of cracking damage to the covered and bare tiles.

The findings suggest that future work should:

1) Confirm findings at higher velocities: Perform tests, analysis and modeling to confirm these findings at higher velocities and for other ceramic targets.
2) Combine modeling and testing to investigate methods to enhance the confinement effect of the cover, for example: i) use covers of different materials and different weaves or construction, ii) vary adhesion between the cover and target, iii) try to develop pre-stress in the tile, e.g., incorporate a fabric that wraps fully around the tile, and iv) use modified target geometries that allow for more effective composite confinement techniques.

Having developed the model, the most efficient approach would be to use the model to study the feasibility of these methods and identify the ones most likely to succeed.

Acknowledgments

The authors would like to thank Terry Henry (SRI International), Paul Zuanich (SRI International), Lasse Sundem-Eriksen (FFI) and Ole Andreas Haugland (FFI) for their technical assistance with the experimental work, and Dr Tom Thorvaldsen (FFI) and Dr John F. Moxnes (FFI) for valuable discussions.

References

[1] Shockey DA, Marchand A, Skaggs S, Cort G, Burkett M, Parker R. Failure phenomenology of confined ceramic targets and impacting rods. Int J Impact Eng 1990;9(3):263–75. doi: 10.1016/0734-743X(90)90002-D.
[2] Lankford J. The role of dynamic material properties in the performance of ceramic armor. Int J Appl Ceram Technol 2004;1:205–10. doi: 10.1111/j.1744-7402.2004.tb00171.x.
[3] Compton BG, Gamble EA, Zok FW. Failure initiation during impact of metal spheres onto ceramic targets. Int J Impact Eng 2013;55(0):11–23. doi: 10.1016/j.ijimpeng.2012.12.002.
[4] Sherman D, Ben-Shushan T. Quasi-static impact damage in confined ceramic tiles. Int J Impact Eng 1998;21(4):245–65. doi: 10.1016/S0734-743 X (97)00063-8.

[5] Sherman D. Impact failure mechanisms in alumina tiles on infinite thickness support and the effect of confinement. Int J Impact Eng 2000;24(3):313–28. doi: 10.1016/S0734-743X(99)00147-5.
[6] Nunn S, Hansen J, Frame B, Lowden R. Improved ballistic performance by using a polymer matrix composite facing on boron carbide armor tiles. Adv Ceram Armor 2005;26(7):287–92.
[7] Sarva S, Nemat-Nasser S, McGee J, Isaacs J. The effect of thin membrane restraint on the ballistic performance of armor grade ceramic tiles. Int J Impact Eng 2007;34(2):277–302. doi: 10.1016/j.ijimpeng.2005.07.006.
[8] Crouch IG, Appleby-Thomas G, Hazell PJ. A study of the penetration behaviour of mild-steel-cored ammunition against boron carbide ceramic armours. Int J Impact Eng 2015;80:203–11. doi: 10.1016/j.ijimpeng.2015.03.002.
[9] Tasdemirci A, Tunusoglu G, Güden M. The effect of the interlayer on the ballistic performance of ceramic/composite armors: Experimental and numerical study. Int J Impact Eng 2012;44:1–9. doi: 10.1016/j.ijimpeng.2011.12.005.
[10] Reddy PRS, Madhu V, Ramanjaneyulu K, Bhat TB, Jayaraman K, Gupta NK. Influence of polymer restraint on ballistic performance of alumina ceramic tiles. Def Sci J 2008;58(2):264–74 9th International Symposium on Plasticity and Impact Mechanics, Ruhr Univ Bochum, Bochum, Germany, Aug 21-24, 2007.
[11] Zaera R, Sánchez-Sáez S, Pérez-Castellanos J, Navarro C. Modelling of the adhesive layer in mixed ceramic/metal armours subjected to impact. Compos Part A: Appl Sci Manuf 2000;31:823–33. doi: 10.1016/S1359-835X(00)00027-0.
[12] López-Puente J, Arias A, Zaera R, Navarro C. The effect of the thickness of the adhesive layer on the ballistic limit of ceramic/metal armours. An experimental and numerical study. Int J Impact Eng 2005;32:321–36. doi: 10.1016/j.ijimpeng.2005.07.014.
[13] Horsfall DBuckley. The effect of through-thickness cracks on the ballistic performance of ceramic armour systems. Int J Impact Eng 1996;18(3):309–18. doi: 10.1016/0734-743X(96)89051-8.
[14] Lundberg P, Renström R, Lundberg B. Impact of conical tungsten projectiles on flat silicon carbide targets: transition from interface defeat to penetration. Int J Impact Eng 2006;32:1842–56. doi: 10.1016/j.ijimpeng.2005.04.004.
[15] Woodward R, W. Jr G, O'Donnell R, Perciballi W, Baxter B, Pattie S. A study of fragmentation in the ballistic impact of ceramics. Int J Impact Eng 1994;15:605–18. doi: 10.1016/0734-743X(94)90122-2.
[16] Crouch IG. Effects of cladding ceramic and its influence on ballistic 28th international symposium on ballistics; 2014. p. 1084–94.
[17] Oberg E, Dean J, Clyne T. Effect of inter-layer toughness in ballistic protection systems on absorption of projectile energy. Int J Impact Eng 2015;76(0):75–82. doi: 10.1016/j.ijimpeng.2014.09.006.
[18] Bürger D, de Faria AR, de Almeida SF, de Melo FC, Donadon MV. Ballistic impact simulation of an armour-piercing projectile on hybrid ceramic/fiber reinforced composite armours. Int J Impact Eng 2012;43:63–77.
[19] Fawaz Z, Zheng W, Behdinan K. Numerical simulation of normal and oblique ballistic impact on ceramic composite armours. Compos Struct 2004;63(34):387–95. doi: 10.1016/S0263-8223(03)00187-9.
[20] Feli S, Asgari M. Finite element simulation of ceramic/composite armor under ballistic impact. Compos Part B: Eng 2011;42:771–80.
[21] Grujicic M, Pandurangan B, d'Entremont B. The role of adhesive in the ballistic/structural performance of ceramic/polymer-matrix composite hybrid armor. Mater Des 2012;41(0):380–93. doi: 10.1016/j.matdes.2012.05.023.
[22] Simha CM, Bless S, Bedford. A. Computational modeling of the penetration response of a high-purity ceramic. Int J Impact Eng 2002;27:65–86.
[23] Johnson GR, Holmquist TJ. An improved computational constitutive model for brittle materials. High pressure science & technology. New York: AIP Press; 1994. p. 981–4.
[24] Lee M, Yoo Y. Analysis of ceramic/metal armour systems. Int J Impact Eng 2001;25:819–29.
[25] Riedel W, Hiermaier S, Thoma K. Transient stress and failure analysis of impact experiments with ceramics. Mater Sci Eng: B 2010;173:139–47.
[26] Eghtesad A, Shafiei A, Mahzoon M. Predicting fracture and fragmentation in ceramic using a thermo-mechanical basis. Theor Appl Fract Mech 2011;56:68–78.
[27] Espinosa H, Dwivedi S, Zavattieri P, Yuan G. A numerical investigation of penetration in multilayered material/structure systems. Int J Solids Struct 1998;35:2975–3001.
[28] Espinosa HD, Zavattieri PD, Dwivedi SK. A finite deformation continuum discrete model for the description of fragmentation and damage in brittle materials. J Mech Phys Solids 1998;46:1909–42.
[29] Thorvaldsen T, Johnsen BB, Jones TP, Rahbek DB, Kawashita LF. Experimental and numerical analysis of peel failure between alumina ceramics and glass fibre-reinforced composites. In: Proceedings of the 20th international conference on composite materials; 2015.
[30] Johnson GR, Cook WH. A constitutive model and data for metals subjected to large strains, high strain rates and high temperatures. In: Proceedings: seventh international symposium on ballistics, 21; 1983. p. 541–7.
[31] Johnson GR, Cook WH. Fracture characteristics of three metals subjected to various strain, strain rates, temperatures and pressures. Eng Fract Mech 1985;21(1):31–48.
[32] "LS-DYNA Keyword User's Manual, Volume 1," Livermore software technology corporation (LSTC) 10/23/14 (r:5792) 2014.
[33] Cronin DS, Bui K, Kauffman C, McIntosh G, Berstad T. Implementation and validation of the Johnson–Holmquist ceramic Model. LS-Dyna 4th European LS-Dyna users conference; 2003.
[34] Malvar, LJ, Crawford, JE, Morrill, KB, K&C concrete material model release III—automated generation of material model input, K&C Technical Report TR-99-24-B1, 18 August 2000 (Limited Distribution).
[35] Lausund KB, Johnsen BB, Rahbek DB, Hansen FK. Surface treatment of alumina ceramic for improved adhesion to a glass fibre-reinforced polyester composite. Int J Adhes Adhes 2015;63:34–45.